

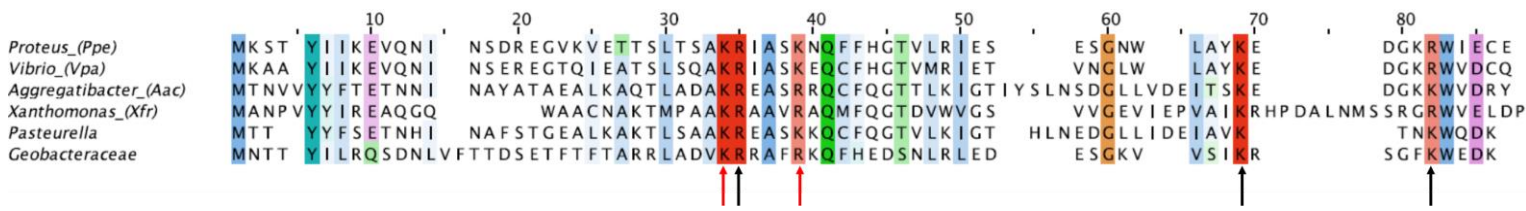
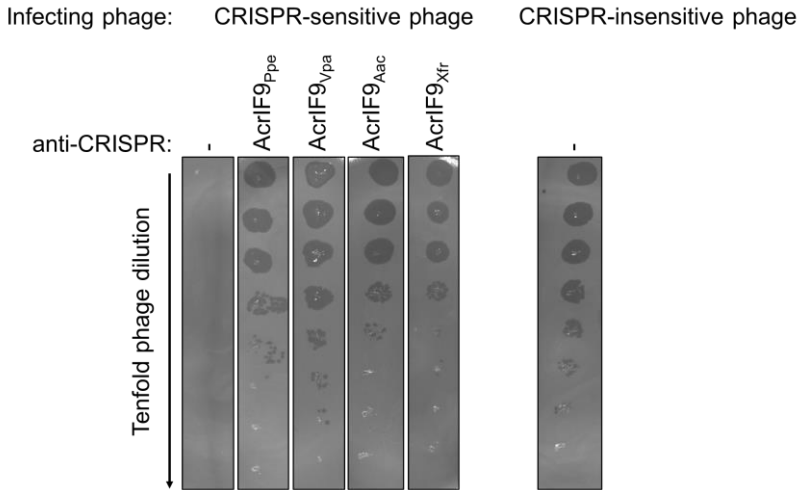
A**B**

Fig S1. AcrIF9 homologues inhibits the *P. aeruginosa* type I-F CRISPR-Cas system. (A) A sequence alignment of 7 diverse members (average pairwise sequence identity = 34%) of the AcrIF9 family. The alignment is colored by conservation according to the ClustalX scheme. The conserved positively charged positions are red. Important residues making up the positive surface are indicated with arrows (black) and those mutated in this study are indicated with red arrows (R32, K36). The sequences shown are PROPEN_01997 (*Proteus penneri* ATCC 35198), D5E77_24790 (*Vibrio parahaemolyticus*), FXB80_00875 (*Aggregatibacter actinomycetemcomitans*), PD5205_04008 (plasmid) (*Xanthomonas fragariae*), BGK37_12565 (*Pasteurella multocida*), JT06_19085 (*Desulfobulbus* sp. Tol-SR), and A2076_14270 (*Geobacteraceae* GWC2_53_11). (B) Dilutions of CRISPR-sensitive (DMS3m) and CRISPR-insensitive bacterium (DMS3) phage lysates were spotted onto lawns of *P. aeruginosa* strain PA14, which has an active type I-F CRISPR-Cas system. PA14 was transformed with plasmids expressing the indicated AcrIF9 homologs. Zones of clearing indicate successful phage infection and inhibition of the CRISPR-Cas system. The negative control is a strain carrying only the expression vector.

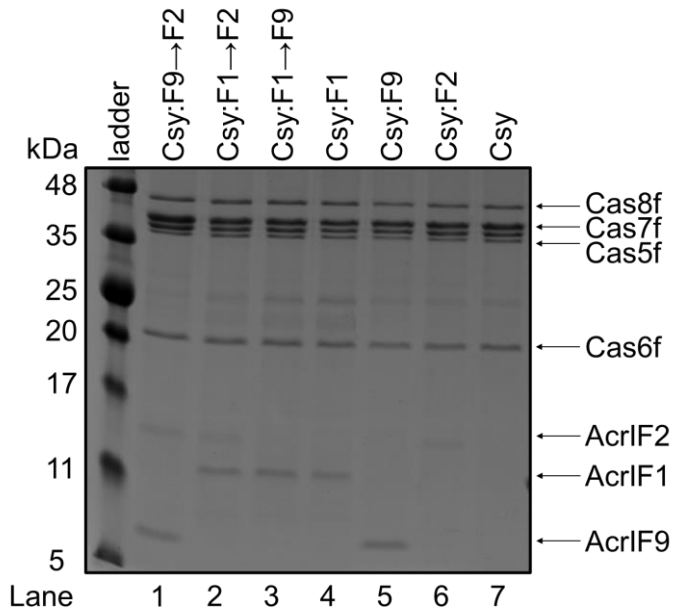


Fig. S2. Competition between Acrs for binding to the Csy complex. Untagged Acrs were mixed with the Csy complex containing 6xHis-tagged Cas7f. The samples were then affinity purified using Ni-NTA beads to remove unbound Acr and proteins eluted from the beads. The samples were visualized on Coomassie Blue stained SDS-PAGE gels. In competitive binding experiments the Acr following the (→) was added second after preincubation with the first Acr.

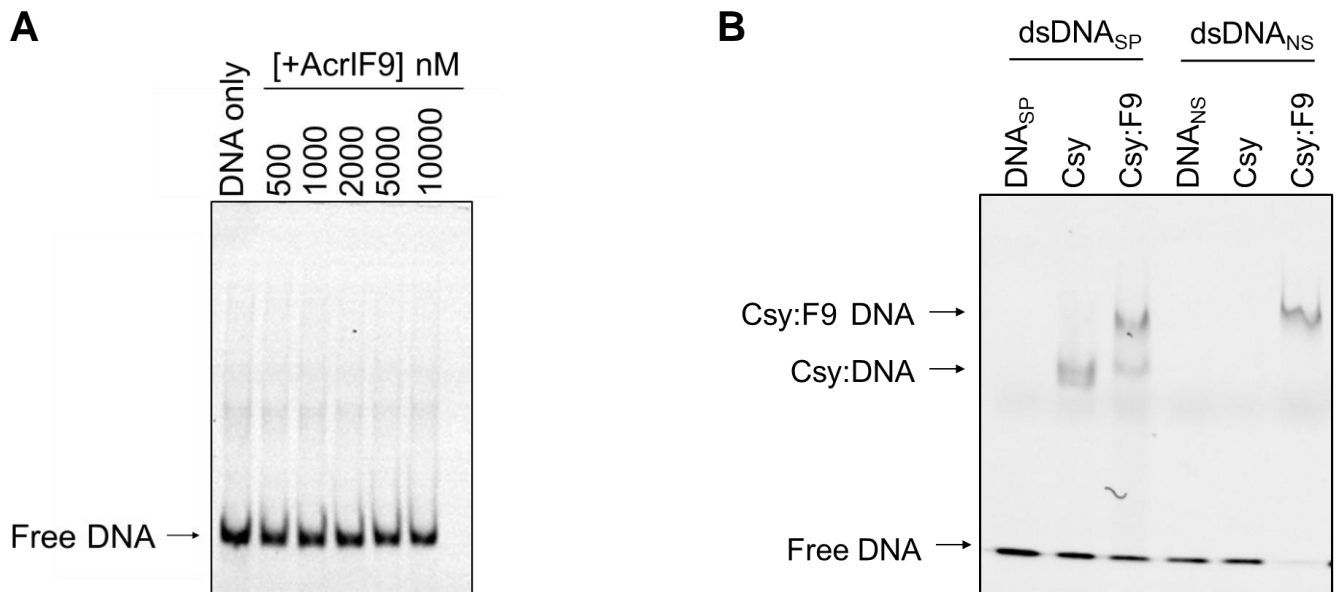


Fig. S3. (A) AcrIF9 does not bind dsDNA without the Csy complex. Increasing concentrations of AcrIF9 were mixed with 100 nM of FAM-6 labeled 50 bp dsDNA_{SP} fragment. No Csy complex was present. DNA binding was detected by EMSA. (B) Csy:F9:DNA complexes were electrophoresed on 4% polyacrylamide gels rather than the 6% gels used in all other experiments. Csy or Csy:F9 complexes were incubated with either dsDNA_{SP} or dsDNA_{NS} and the samples were separated under the same condition as in other EMSA experiments.

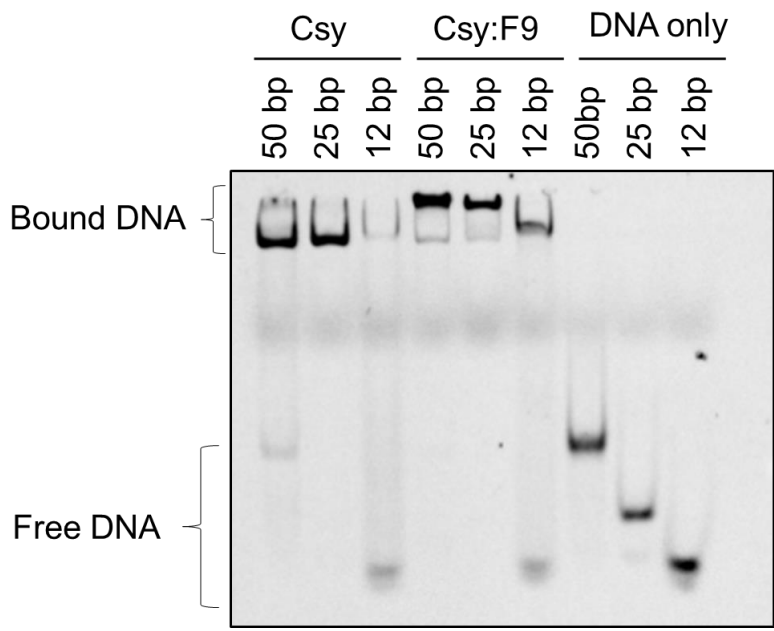


Fig. S4. Binding of Csy:F9 to shorter length dsDNA_{SP} targets. EMSA gel showing the binding of Csy or Csy:F9 complexes to 50, 25, 12 bp complementary dsDNA.

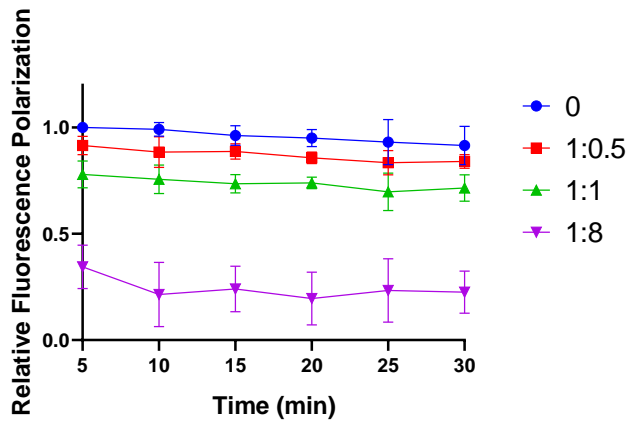
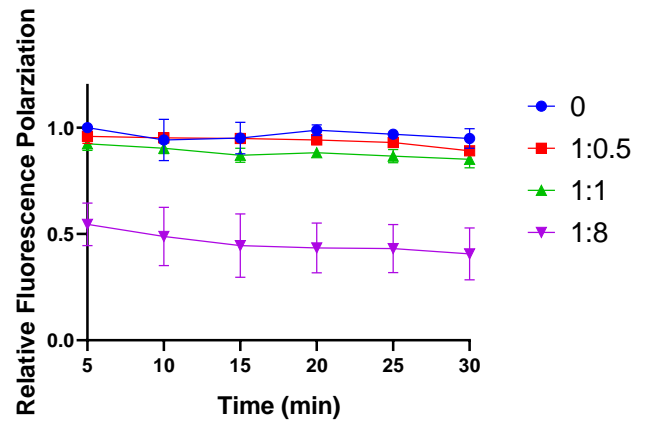
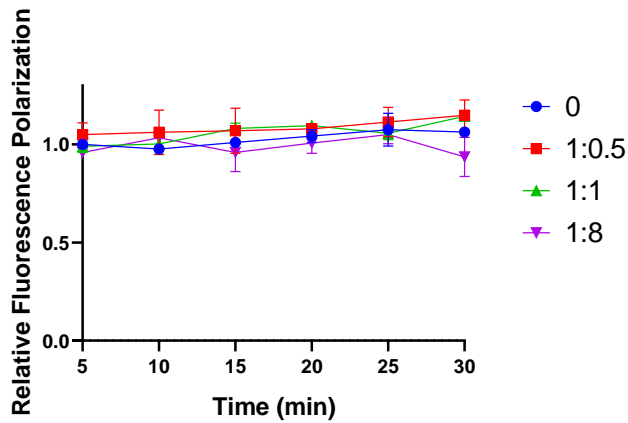
A**B****C**

Fig. S5. The dsDNA bound by Csy:F9 is rapidly competed off. Csy or Csy:F9 complexes were pre-saturated with Cy5-labeled DNA, then increasing concentrations of unlabeled DNA were added at levels ranging from 0.5 to 8-fold excess over the concentration of the labeled DNA (i.e. ratios of 1:0.5, 1:1, 1:8). FP measurements were taken at various times after addition of the unlabeled DNA. Due to limitations of the apparatus being used, time points shorter than 5 min could not be assayed. Relative fluorescence polarization was calculated using the ratio of the values from each competitor concentration to that without competitor DNA at 5 min. All error bars represent SD, $n = 3$. (A) Csy:F9 was pre-saturated with dsDNA_{SP} and competed with unlabeled dsDNA_{NS}. (B) Csy:F9 was pre-saturated with dsDNA_{NS} and competed with unlabeled dsDNA_{SP}. (C) Csy complex was pre-saturated with dsDNA_{SP} and competed with unlabeled dsDNA_{SP}.

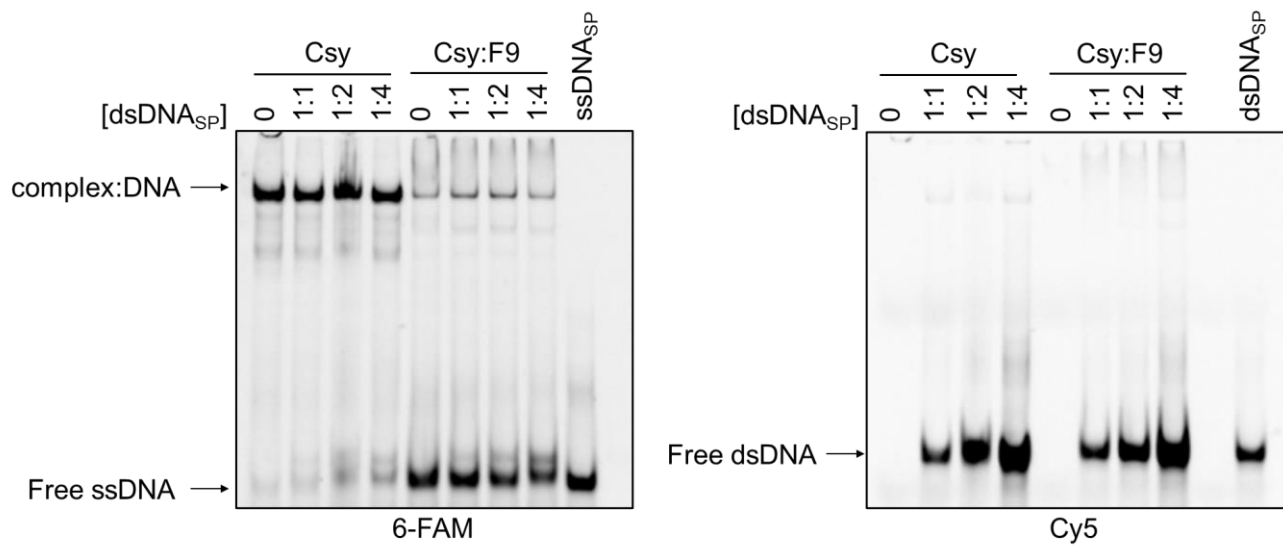


Fig. S6. Csy:F9 differentially interacts with dsDNA and ssDNA. Csy or Csy:F9 complexes (2000 nM) were pre-saturated with 1000 nM of 6-FAM labeled ssDNA_{SP}, then increasing concentrations of Cy5-labeled dsDNA_{SP} were added as competitor. DNA-binding was monitored by EMSA. The ratio of dsDNA_{SP} to dsDNA_{NS} is shown over each lane. The same gel was irradiated at 473 nm to visualize the 6-FAM-labeled DNA (left panel) and at 673 nm to visualize the Cy5-labeled DNA (right panel).

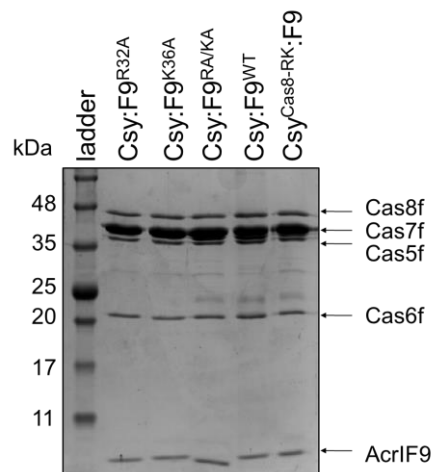
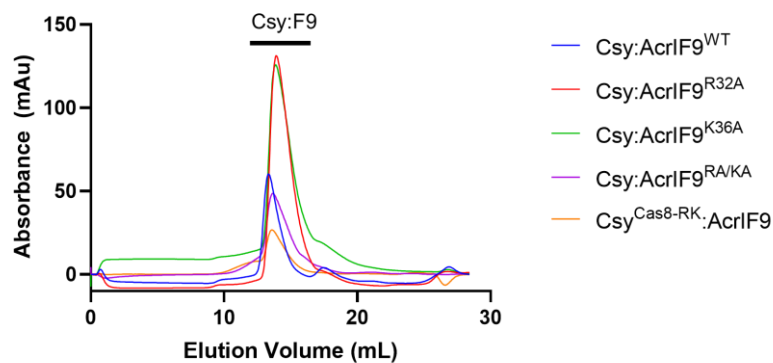
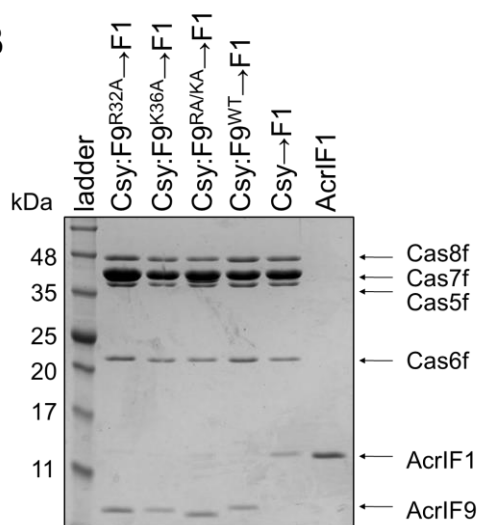
A**B**

Fig. S7. Csy complexes by to AcrIF9 mutants purify normally and the mutants remain bound to the Csy complex through purification. (A) Size-exclusion chromatography (Superdex 200 10/30, GE Healthcare) profile and SDS-PAGE analysis of the Csy complex copurified with the AcrIF9 mutants (F9^{R32A}, F9^{K36A}, F9^{RA/KA}) and Csy^{Cas8-RK}:F9. (B) Competition of AcrIF1 to AcrIF9 mutants co-purified with the Csy complex. 6xHis-tagged Csy:F9^{WT} or Csy bound to F9 mutants (F9^{R32A}, F9^{K36A}, F9^{RA/KA}) were incubated with 10x molar excess of untagged AcrIF1 for 1 hour. The samples were then affinity purified using Ni-NTA beads to remove unbound Acr and proteins eluted from the beads. The samples were visualized on Coomassie Blue stained SDS-PAGE gels. The (→) indicate that AcrIF1 was added as a competitor.

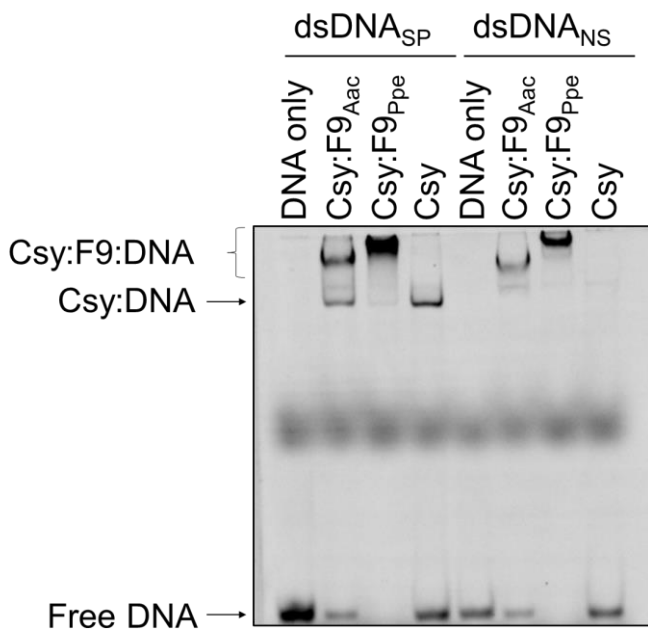


Fig. S8. Non-specific DNA binding is a conserved feature of AcrIF9 homologues. EMSA gels showing binding of Csy:F9_{Aac}, Csy:F9_{Ppe}, and Csy alone to Cy5-labeled dsDNA_{SP} and dsDNA_{NS}. These experiments were performed under identical conditions as those shown in Fig. 1A.

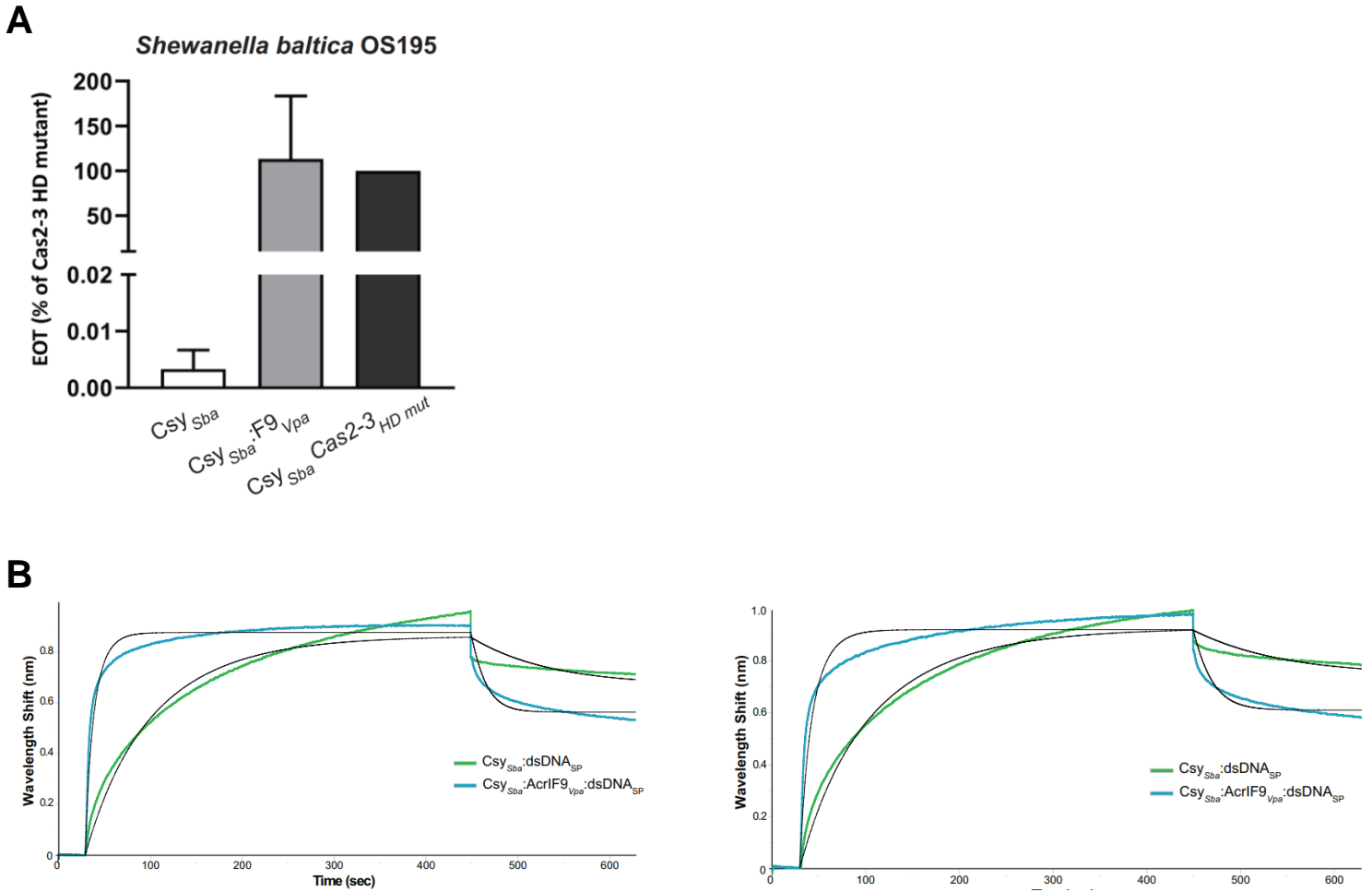


Fig. S9. AcrIF9 inhibits the Type I-F system of *S. baltica* (Csy_{Sba}). (A) Efficiency of Transformation assays (EOTs) of the Csy_{Sba} complex expressed in *E. coli* BL21-AI were performed. The activity of the effector complexes was tested when expressed alone (Csy_{Sba}) or co-expressed with AcrIF9_{Vpa}. EOT is equal to the colony ratio between the strain of interest and its corresponding Cas2-3 HD mutant strain, presented as percentages. Error bars represent the SEM, three replicates were quantified. (B) Independent BLI wavelength shifts (nm) generated by the binding Csy_{Sba} to a specific dsDNA oligonucleotide, in the presence (blue) or absence (green) of AcrIF9_{Vpa} are shown. Each experiment was performed with independently purified protein samples and freshly diluted oligonucleotide stocks. Non-linear regressions obtained by least-square fit by the BLItz Pro Software are shown in black for each curve.

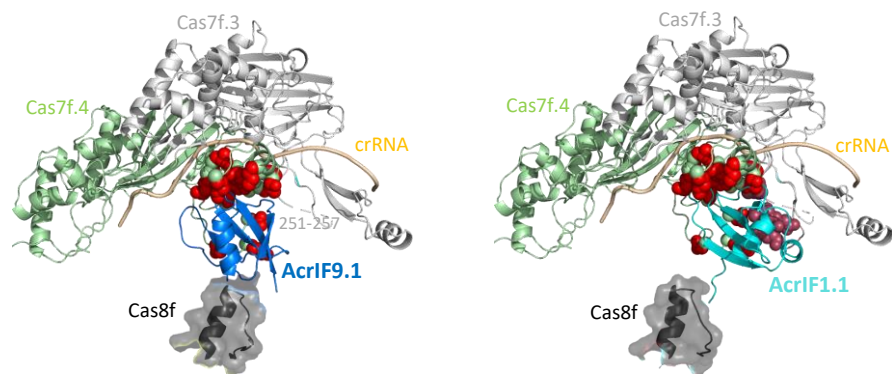


Fig. S10. Features of the interactions of AcrIF9 and AcrIF1 with the Csy Complex. (A) The interaction interfaces of AcrIF9.1 (left) and AcrIF1.1 (right) with the Csy complexes are shown. Residue side chains in Cas7f.4 that interact with both AcrIF9.1 and AcrIF1.1 are shown in red. When bound to AcrIF9.1, a loop in Cas7f.4 (residues 251-257) indicated in the left panel is disordered. When AcrIF1.1 is bound this loop is ordered and forms intersubunit bridging interactions. Cas7f.4 residues in this interface from the AcrIF1 bound Csy complex (PDB ID 5UZ9) are shown in dark red in the right panel. These figures were made by overlaying the Cas7f subunits of the AcrIF1 bound and AcrIF9 bound (PDB ID 6VQV) structures. These subunits overlay with less than 2 Å root mean square deviation.